

FORMING LIMIT DIAGRAM, VOID ANALYSIS, STRAIN DISTRIBUTION AND SURFACE ROUGHNESS FOR SS430 SHEETS DURING MULTIPOINT INCREMENTAL FORMING

Single point incremental forming process is a most economical Die-less forming process. The major constraint of it is that it is a time consuming process. In this work, a new attempt was made in incremental forming process using Multipoint tool for SS430 sheets to increase the formability and to reduce forming time. Fractography analysis was made to study the size of voids that were formed during fracture. The forming limit diagrams were drawn and compared for single point incremental forming and the multipoint incremental forming of SS430 sheet. It was proved that the formability of SS430 sheet in the multipoint forming was better than the formability of that in single point forming and the time consumed was reduced. The strain distribution in both processes had also been studied along with surface roughness.

Keywords: FLD, SPIF, MPIF, Void coalescence, Strain distribution

1. Introduction

Incremental sheet metal forming (ISF) which is a cost effective process is deployed in industries to make prototype using CNC machine. The single point and two point incremental forming processes are the two methods that are successfully followed so far [1]. The tool used for single point incremental forming (SPIF) is simple in construction but, the process consumes more time, which made the SPIF unsuitable for mass production [2]. Contour shapes can be formed by ISF using a hemispherical ended tool or by attaching a hardened steel ball to the end of tool shank, which are controlled by CNC program [2,3]. In spite of its high tool speed with a high feed rate, ISF consumes more time than that of a conventional forming process and still SPIF is being utilized in rapid prototyping due to its cost effectiveness [4]. In SPIF, feed, speed and vertical step depth of tool influences the formability of material being formed and also its accuracy. Lubrication between the sheet material and tool interface determines the surface quality of the formed product. Another criterion of the formability of the sheet is the wall angle in which Hirt et al. [5] had made an attempt on mild steel and Al to overcome the limitations of getting maximum wall angle and inhomogeneous thickness distribution. Ambrogio et al. [6], attempted to increase the dimensional accuracy of AA1050-O that is formed by SPIF and comparing the experimental results with analytical results. Raju et al. [3] arrived at a better formability in commercially pure copper sheets using multi sheet SPIF. From the literature survey it is found that the incremental

forming has been used mostly for materials like aluminium and copper [2,7] was used. In the present study, stainless steel (SS) 430, which is a ferritic, chromium, non-hardenable grade with better formability is incrementally formed. The SS430 exhibits an excellent resistance to stress corrosion cracks, pitting and crevice type of corrosions. The presence of chromium in the SS430 grade enhances the oxidation and corrosion resistance and resists scaling (oxidation) even at elevated temperatures (816°C). The existence of low nickel percentage in SS430 grade reduces the cost without compromising its mechanical properties. The SS430 grade shows low strain hardening rate, which enables the steel to be readily formed by any metal working process. The above mentioned traits, paved a path for the application of SS430 grade sheets in house hold appliances (namely, refrigerator and sink), architectural and automotive trims. However, all these applications involve the sheet metal of SS430 grade, which are plastically deformed by any metal forming process without failure. Though reports are available on single point incremental forming (SPIF), the influence of various process parameters on SS430 using multipoint incremental forming (MPIF) is lagging. The main significance of MPIF tool is that it increases the formability since more contact area is made with the sheet which improves the wall angle of the material and the forming time of the process is also highly reduced. In this investigation, an attempt is made to incrementally form a SS430 grade sheet metal by both SPIF and MPIF and to study the strain distribution and formability of the material through forming limit diagram and void coalescence analysis.

* DHANALAKSHMI SRINIVASAN INSTITUTE OF TECHNOLOGY, DEPARTMENT OF MECHANICAL ENGINEERING, TRICHY-621112, TAMILNADU, INDIA.

** SHIVANI COLLEGE OF ENGINEERING AND TECHNOLOGY, DEPARTMENT OF MECHANICAL ENGINEERING, TRICHY-620009, TAMILNADU, INDIA.

*** SRINIVASAN ENGINEERING COLLEGE, DEPARTMENT OF MECHANICAL ENGINEERING, PERAMBALUR-621212, TAMILNADU, INDIA.

**** NATIONAL INSTITUTE OF TECHNOLOGY, DEPARTMENT OF PRODUCTION ENGINEERING, TRICHY-620015, TAMILNADU, INDIA.

Corresponding author: csathiya@nitt.edu

2. Material chemical composition, microstructure and experimentation

The Stainless steel (SS) 430 was procured and the thickness of sheet used is 0.4 mm since at this thickness stainless steel can be worked easily using standard tools and Equipment's. The chemical composition of the SS430 sheet used is determined by spectrometry and it is presented in Table 1. The microstructure of SS430 was observed as per standard metallography test which is shown in Fig. 1.

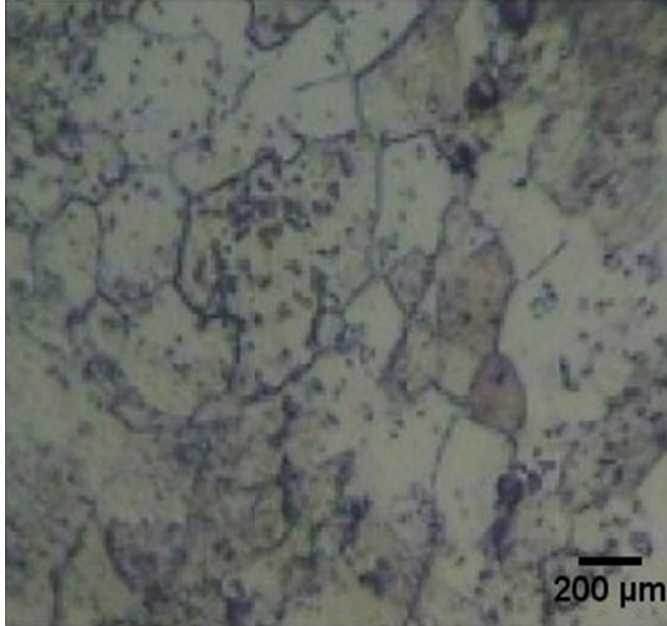


Fig. 1. Microstructure of SS430

The tensile test as per the standard ASTM E08 was also conducted using UTM. The samples for the Tensile test were cut using laser cutting as shown in Fig. 2.

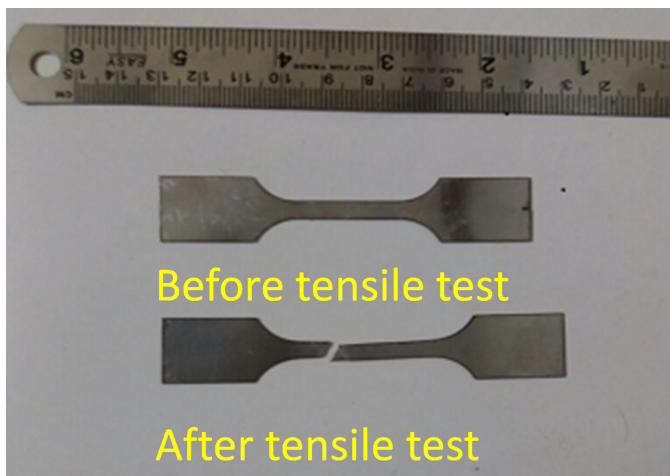


Fig. 2. Tensile Test Specimen as per ASTM E08 Standard

The true stress and True strain curve was plotted, as shown in Fig. 3. The blanks for incremental forming were sheared to

a dimension of 150 mm × 150 mm. The blank was fixed on a milling fixture. By using SPIF and MPIF tools with ball diameter 12.7 mm the forming operation was carried out using a vertical CNC machining centre by varying the process parameters namely, speed, feed rate, vertical step depth and lubrication.

TABLE 1

Chemical composition of SS430 sheet

Composition	Percentage (%)
C	0.017
Mn	0.917
Cr	12.11
Ni	0.269
Si	0.410
S	0.008
P	0.023
Mo	0.013

The speed of the tool were varied as 100 rpm, 150 rpm and 200 rpm ; the feed rate were varied as 50 mm/min, 100 mm/min and 150 mm/min; the vertical step depths were kept as 0.1 mm, 0.2 mm and 0.3 mm. Furthermore, the lubrication media used were dry, oil and grease.

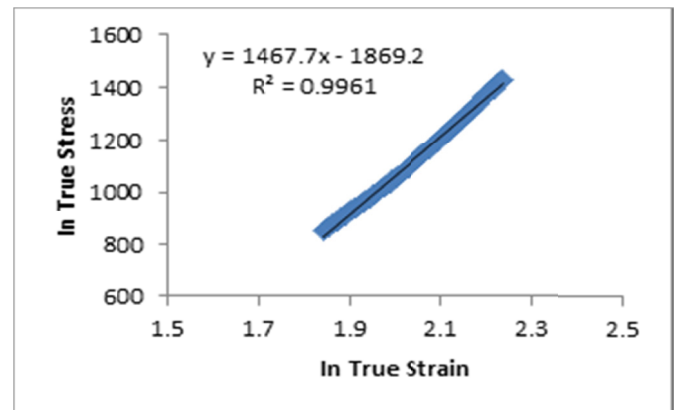


Fig. 3. True Stress Vs True Strain curve for SS430 sheet

Hyperbolic shape [8] is made with various wall angles as shown in Fig. 4. The circular grids were made on the blank using laser markings. From which the major and minor diameters of the deformed circular grids were measured by using Video measuring machine named Tesa Microhite 3D with accuracy ±5 micrometer. Major and minor true strain values are obtained as explained elsewhere[9] with which the forming limit Diagrams were plotted by taking major true strain in Y-axis and minor strain in X-axis and compared between the SPIF and MPIF. The strain distribution curves were also plotted for both SPIF and MPIF by taking distance from centre of cup in X-axis and strain in Y-axis. The fracture surfaces were also observed using the scanning electron microscope, void sizes were observed analysis on this was done. The surface roughness was also measured from which 2d-surface roughness graph along with 3d-image of the surface formed was obtained.

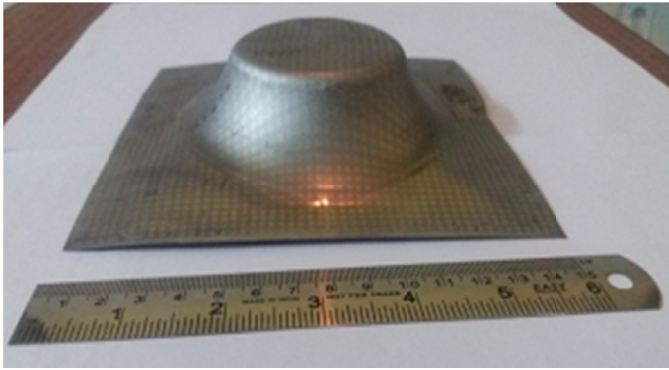


Fig. 4. Formed cup using MPIF

3. Results and discussion

3.1. Chemical composition, Microstructure and Tensile properties

The chemical composition of the SS430 sheet taken for study is shown in Table 1. The content of Nickel and chromium which reduces the brittleness of the SS430 [17] and the presence of chromium increases the strength and act as a corrosion resistant which make its application more in automotive industries. The microstructure of SS430 shown in Fig. 1 shows the ferritic coarse grains with carbide particles. The Ferritic grains gives more formability to the sheet metal [12]. The Tensile test with details of the material deforms in the Engineering stress range of 90-172 Mpa and engineering strain range of 1.32 to 18.6%. The strain hardening exponent (n) was also calculated from the log-log graph using the true stress (σ) and true strain (ϵ) plot as 0.45.

3.2. Forming Limit Diagram

Forming limit diagram (FLDs) were plotted for the true strain values obtained, by considering the major true strain ϵ_1 values along the X-axis and minor true strain ϵ_2 values along the Y-axis as shown in Fig. 5. From the graph it is evident that the major true strain values of the multipoint tool is higher when compared to the major true strain values of single point tool for the corresponding minor true strain values. In the FLD, for a given minor true strain value of 0, the major true strain values of multipoint tool is noted to be higher (major true strain = 0.95) than that of single point tool (major true strain = 0.7) which is 24% higher which is shown in Table 2. This is due to [8] the proneness of sheet failure is less when larger diameter balls are deployed when compared to smaller ball diameter in AA1050. This is attributed to the enhanced concentration of smaller ball at a particular area of sheet had resulted an early damage to the sheet. Joost Duflou et al. [10] and Yanle li et al. [11] also made similar attempt on AA 3103 and AA 7075 and inferred better formability in SPIF having larger ball diameter. Also axial forming force can be increased with maximum tool

diameter which improves the Formability of the sheet in less time with reduced friction [19]. As in the case of SS430, it holds better formability due to ferrite grains and in addition, the maximum amount of chromium content also enhances the formability of SS430 [12] to produce cup and cone fracture which is usually formed in ductile material as shown in Fig. 6. Tyler et al. [13] had also made attempt to prove that by varying the edge radius the forming characteristics of the metal can be improved because the perpendicular force created on the sheet while forming operation using single point tool increases the friction on a particular point. Whereas in MPIF the tool deforms more contact surface with more number of ball movement than SPIF thus reducing the friction between the ball and the sheet thus reduces the thinning of the material which leads to fracture. when the friction is reduced the wear rate of the tool is also reduced thus giving good surface finish. The formability of the material may also increase due to the von-mises stress [14] which increase the yield strength of the material while using MPIF. The yield strength is increased due to more surface contact between the work piece and the tool by reducing the strain rate which causes the deformation [15].

TABLE 2

Comparison of Minor Strain With Major Strain for SPIF and MPIF

Minor strain	Major strain		Increase in major strain in%
	SPIF	MPIF	
0.0	0.69	0.93	24%
0.1	0.6	0.84	24%
0.2	0.5	0.74	24%

Due to yield strength, material flows from un-deformed material by reducing thinning of the material at early stage which gives more formability [13]. Therefore more surface contact in MPIF may lead the load to be tensile in nature rather than compressing at a point which improves the formability by giving higher wall angle.

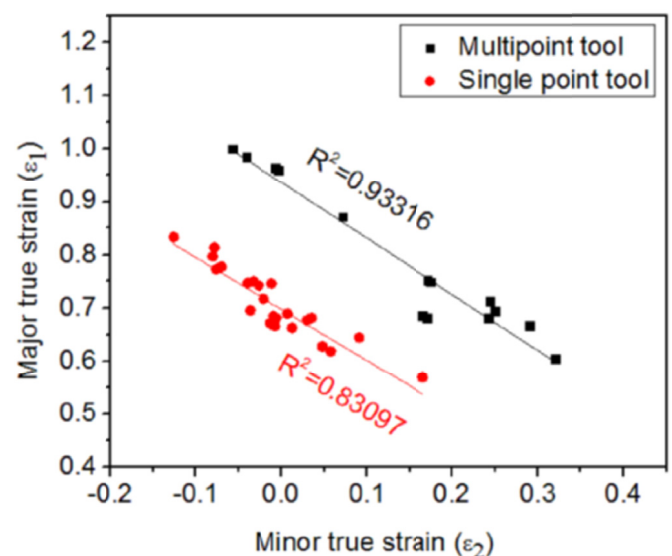


Fig. 5. FLD for SPIF and MPIF

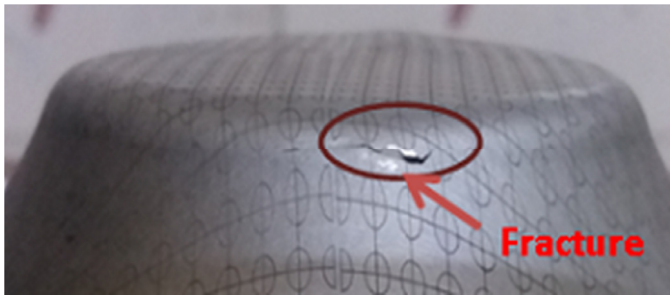


Fig. 6. Fracture obtained while Forming

surface resulting in better formability. Similarly, in the present work using MPIF tool having more number of balls results better formability than the SPIF Tool.

3.4. Strain distribution profile

The strain distribution has made along the steel as shown in Fig. 9 and strain distribution profile for MPIF and SPIF were plotted as shown in Fig. 10. In this operation it is observed that

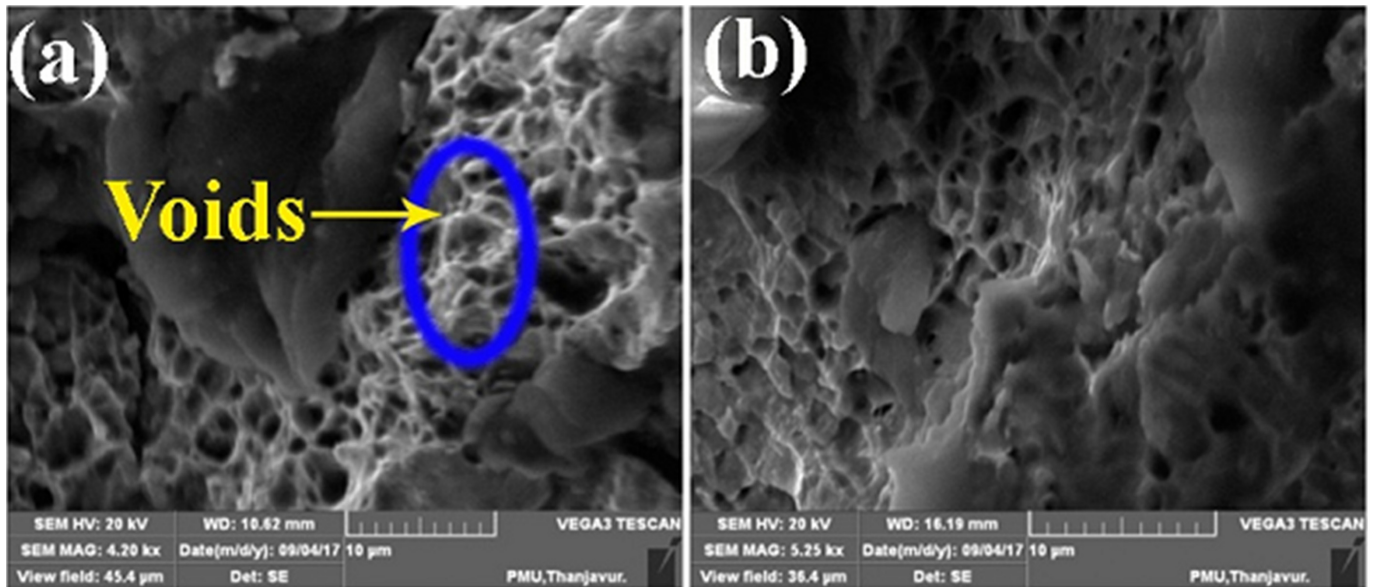


Fig. 7. Fractographs of (a) MPIF and (b) SPIF

3.3. Void coalescence

In order to obtain better understanding of formability the Fractographic analysis was made on the specimens and the void growth were analysed using the void coalescence parameters [16]. Void analysis test helps us to check the plastic deformation the material undergoes which is an indirect measure of formability of the sheet. In which the void circumference formed is measured and compared between the SPIF and MPIF. The Fractographs of MPIF and SPIF are shown in Fig. 7a,b respectively. In MPIF Fractographs it is noticed that more number of voids are formed than the SPIF. Since the number of voids affects the formability of the work piece [17] the Void circumference and L/W ratio are taken as parameters to calculate the void coalescence. From the values calculated the void circumference and L/W ratio values of MPIF seems to be higher in size than the void circumference of the SPIF as shown in Fig. 8. The higher void circumference indicates a good formability of multipoint incremental tool which is due to the more contact surface between the tool and the sheet.

This proves that the void increases as the effective strain increase [18] which is maximum for MPIF than SPIF as shown in FLD Fig. 5. Similar process was done in various ball diameter [19] in which ball with maximum diameter has more contact

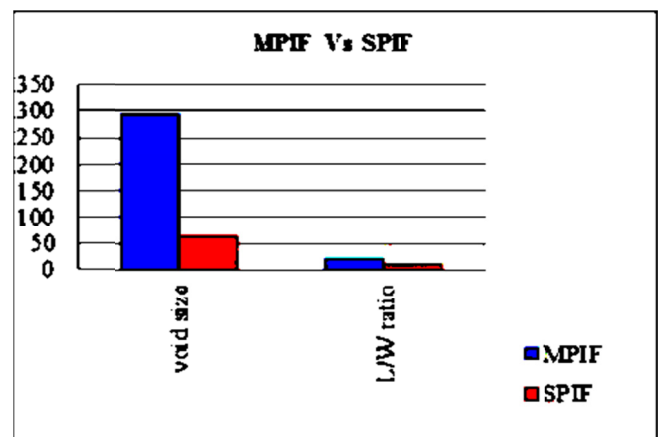


Fig. 8. Comparison of Void circumference and L/W ratio between SPIF and MPIF

the difference in strain at peak obtained using MPIF is higher than the SPIF. When the sheet is subjected to MPIF the major strain exhibits tension while the minor strain undergoes Compression which shows that the ductility of the material increases while undergoing the Tension-Compression in the forming region [20]. Similarly when the sheet is deformed using SPIF the major and minor strain both the strain undergoes tension. Thus tension-tension region is created in the forming region thus reducing

the strain difference between the major and minor strain. This may be due to the force produced by the tool compress the sheet perpendicular to the sheet and not along the wall of the formed cup. This creates the fracture at the earlier stage in SPIF than MPIF. Thus when the minor strain is compressive in nature the sheet becomes tensile which improves the formability while formed using MPIF.

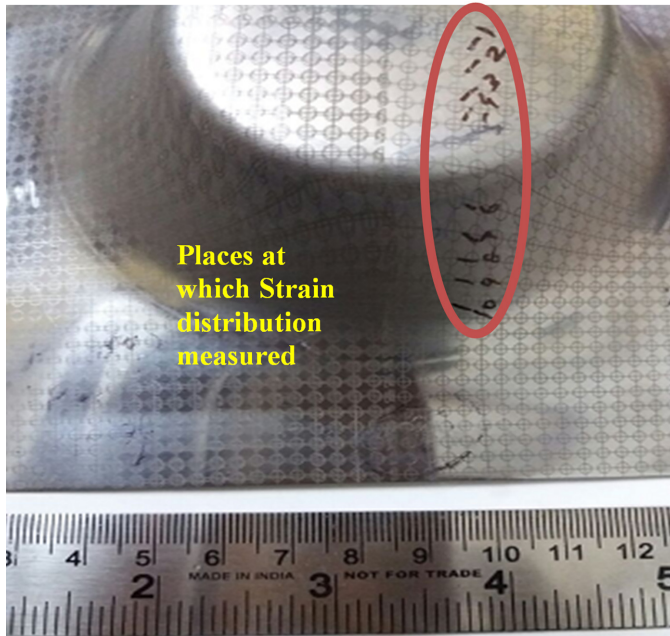


Fig. 9. Image representing the Strain distribution measured

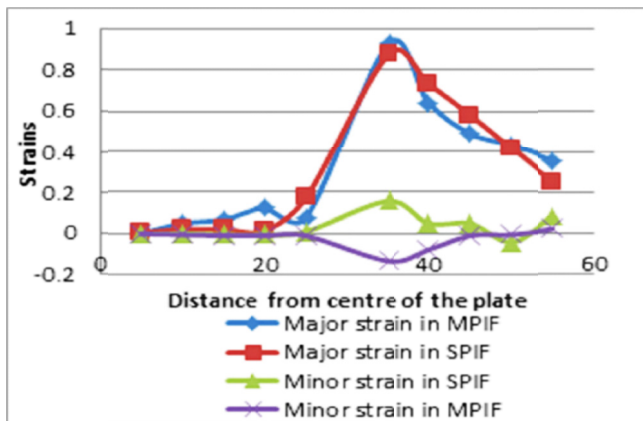


Fig. 10. Major Strain and minor strain distribution in SPIF and MPIF

3.5. Surface roughness

Surface roughness produced in the forming operation is one of the important performances measured. The SPIF generates the surfaces having more roughness than the surface produced by the MPIF. It is analysed using the Non-contact surface roughness Tester named as TALYSURF CCI (coherence correlation interferometry) LITE for both components formed by SPIF and MPIF. The 2d-surface roughness profile obtained shows that peaks and valleys in surface produced by SPIF shown in Fig. 11a

is more than the surface produced by MPIF as in Fig. 11b. Also the Arithmetic mean deviation roughness profile (R_a) of MPIF is obtained as 0.427 and for SPIF it was 0.610 which is higher than MPIF.

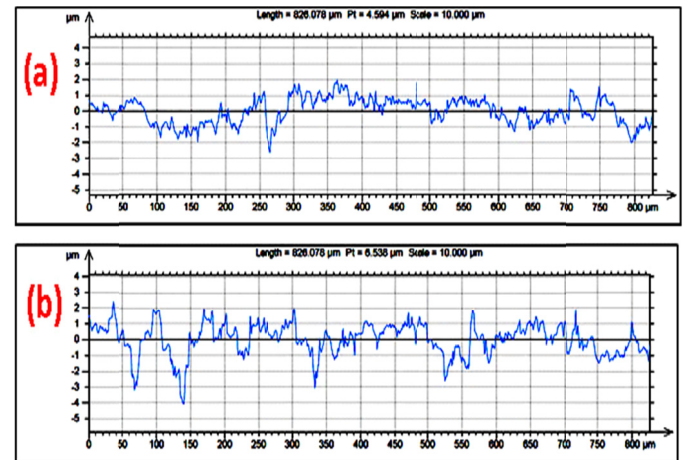


Fig. 11. Roughness profile measured on the surface of (a) MPIF and (b) SPIF

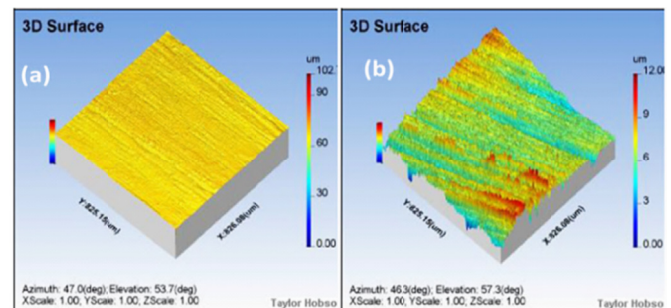


Fig. 12. 3d-Image measured on the surface of (a) MPIF & (b) SPIF

The 3d surface of the formed sheet is shown in Fig. 12 in which the red colour indicates higher roughness which is visible more in SPIF. The reason for the above may be due to that in SPIF a ball compresses a particular point on the path created while forming only once whereas in multipoint forming more number of balls are used to compress the particular point on the sheet to form a component. since the number of passes are increased the balls overlap the gouges (intendation) formed on the surface thus the surface gets smoother when compared to the SPIF [21].

4. Conclusion

In this paper, the formability of the SPIF and MPIF is compared using FLD and found that the formability of the MPIF tool was higher than the SPIF. From the Fractographs test it was found that more number of voids are observed in the multipoint forming rather than single point forming and also void coalescence analysis was used to prove that the higher void circumference obtained through MPIF indicating better formability through MPIF tool due to higher contact area and

sheet interface. The strain distribution curve is also plotted with major strain and minor strain values for the sheets formed by SPIF and MPIF. While comparing both the strain distribution values it is found that the MPIF forming gives better formability. The surface roughness is also reduced in MPIF due to increase in the number of balls which compress the peaks produced on the surface during the forming process.

REFERENCES

- [1] L. Zhaobing, L. Yanle, A.M. Paul, *Mater. Manuf. Process.* **28**, 562-571 (2013).
- [2] G. Ambrogio, V. Cozza, L. Filice, F. Micari, *J. Mater. Process. Technol.* **191**, 92-95 (2007).
- [3] C. Raju, C. Sathiyarayanan, *Measurement.* **78**, 296-308 (2016).
- [4] C. Radu, *J. Eng. Stud. Res.* **17/3**, 71-74 (2011).
- [5] G. Hirt, J. Ames, M. Bambach, R. Kopp, *CIRP Annals-Manuf. Technol.* **53**, 203-206 (2004).
- [6] G. Ambrogio, I. Costantino, L. De Napoli, L. Filice, L. Frantini, M. Muzzupappa, *J. Mater. Process. Technol.* **153-154**, 501-507 (2004).
- [7] C. Raju, C. Sathiyarayanan, *Trans. Ind. Inst. Met.* **69**, 1237-1243 (2016).
- [8] L. Ben Said, J. Mars, M. Wali, F. Dammak, *Int. J. Mech. Sci.* **131-132**, 546-558 (2017).
- [9] V. Mugendiran, A. Gnanavel Babu, *Procedia Eng.* **97**, 1983-1990 (2014).
- [10] D. Joost, T. Yasemin, S. Alex, V. Paul, *J. Mater. Process. Technol.* **189**, 65-72 (2007).
- [11] L. Yanle, L. Zhaobing, W.J.T. Daniel, P.A. Meehan, *J. Mater. Process. Technol.* **29**, 121-128 (2014).
- [12] R. Narayanasamy, C. Sathiyarayanan, *Mater. Sci. Eng., A.* **417**, 197-224 (2006).
- [13] J.G. Tyler, R. Ihab, T.R. John, *Procedia Manufacturing.* **10**, 510-519 (2017).
- [14] G. Hussain, H.R. Khan, L. Gao, N. Hayat, *Mater. Manuf. Processes.* **28**, 324-329 (2013).
- [15] Y.H. Kim, J.J. Park, *J. Mater. Process. Technol.* **130-131**, 42-46 (2002).
- [16] K.S.V.B.R. Krishna, S. Vigneshwaran, K. Chandrasekhar, S.R.S. Akella, K. Sivaprasad, R. Narayansamy, K. Venkateshwarlu, *Int. J. Adv. Manuf. Technol.* **93**, 253-259 (2017).
- [17] K. Pandian, K. Manonmani, *Int. J. Appl. Chem.* **12**, 139-156 (2016).
- [18] Z. Yang, C. Zengtao, *Int. J. Fract.* **143**, 105-112 (2007).
- [19] I. Bagudanch, G. Centeno, C. Vallengano, M.L. Garcia-Romeu, *Procedia Eng.* **63**, 354-360 (2013).
- [20] R. Narayanasamy, C. Sathiyarayanan, *Mater. Des.* **28**, 1555-1576 (2007).
- [21] J.G. Tyler, R. Ihab, T.R. John, *Procedia Manufacturing.* **10**, 520-530 (2017).